Socially Parasitic Ants Evolve a Mosaic of Host-Matching and Parasitic Morphological Traits

Article *in* Current Biology · July 2020

DOI: 10.1016/j.cub.2020.06.078

8 authors, including:

Georg Fischer
Okinawa Institute of Science and Technology
74 PUBLICATIONS **447** CITATIONS
SEE PROFILE

Nicholas R Friedman
Okinawa Institute of Science and Technology
34 PUBLICATIONS **339** CITATIONS
SEE PROFILE

Jen-Pan Huang
Academia Sinica
50 PUBLICATIONS **484** CITATIONS
SEE PROFILE

Nitish Narula
National Institutes of Health
14 PUBLICATIONS **1,172** CITATIONS
SEE PROFILE

Report

Current Biology

Socially Parasitic Ants Evolve a Mosaic of Host-Matching and Parasitic Morphological Traits

Highlights

- A monophyletic group of Malagasy *Pheidole* ants parasitizes congeneric host species
- Host species are not the closest relatives of parasites; Emery's rule does not apply
- 2D and 3D analyses show parasite morphology tends to match their host
- Morphological sensing by hosts is proposed as a selective force (Wasmannian mimicry)

Authors

Georg Fischer, Nicholas R. Friedman, Jen-Pan Huang, ..., Brian L. Fisher, Alexander S. Mikheyev, Evan P. Economo

Correspondence

georgf81@gmail.com (G.F.), evaneconomo@gmail.com (E.P.E.)

In Brief

Fischer, Friedman et al. find an interesting clade of ants that parasitize other, closely related ants from Madagascar. Morphological analyses reveal that parasite morphology evolves to match host morphology, raising questions about the role of morphological sensing in social insect recognition systems.

Fischer et al., 2020, Current Biology *30*, 1–8
September 21, 2020
https://doi.org/10.1016/j.cub.2020.06.078

CellPress

Please cite this article in press as: Fischer et al., Socially Parasitic Ants Evolve a Mosaic of Host-Matching and Parasitic Morphological Traits, Current Biology (2020), https://doi.org/10.1016/j.cub.2020.06.078

Current Biology

CellPress
OPEN ACCESS

Report

Socially Parasitic Ants Evolve a Mosaic of Host-Matching and Parasitic Morphological Traits

Georg Fischer,[1,7,8,*] Nicholas R. Friedman,[1,7] Jen-Pan Huang,[2,3] Nitish Narula,[1] L. Lacey Knowles,[3] Brian L. Fisher,[4] Alexander S. Mikheyev,[5,6] and Evan P. Economo[1,*]

[1]Biodiversity and Biocomplexity Unit, Okinawa Institute of Science and Technology Graduate University, 1919-1 Tancha, Onna, Kunigamigun, Okinawa 904-0495, Japan
[2]Biodiversity Research Centre, Academia Sinica, 128 Academia Road, Section 2, Nankang, Taipei 11529, Taiwan
[3]Museum of Zoology, Department of Ecology and Evolution, University of Michigan, 3600 Varsity Drive, Ann Arbor, MI 48108, USA
[4]Department of Entomology, California Academy of Sciences, Golden Gate Park, 55 Music Concourse Drive, San Francisco, CA 94118, USA
[5]Ecology and Evolution Unit, Okinawa Institute of Science and Technology Graduate University, 1919-1 Tancha, Onna, Kunigamigun, Okinawa 904-0495, Japan
[6]Research School of Biology, Australian National University, 134 Linnaeus Way, Acton, ACT 2601, Australia
[7]These authors contributed equally
[8]Lead Contact
*Correspondence: georgf81@gmail.com (G.F.), evaneconomo@gmail.com (E.P.E.)
https://doi.org/10.1016/j.cub.2020.06.078

SUMMARY

A basic expectation of evolution by natural selection is that species morphologies will adapt to their ecological niche. In social organisms, this may include selective pressure from the social environment. Many non-ant parasites of ant colonies are known to mimic the morphology of their host species, often in striking fashion [1, 2], indicating there is selection on parasite morphology to match the host (Batesian and/or Wasmannian mimicry [3]). However, ants that parasitize other ant societies are usually closely related to their hosts (Emery's rule) [4–8] and expected to be similar due to common ancestry, making any kind of mimicry difficult to detect [9]. Here, we investigate the diversification of the hyperdiverse ant genus *Pheidole* in Madagascar, including the evolution of 13 putative social parasite species within a broader radiation of over 100 ant species on the island. We find that the parasitic species are monophyletic and that their associated hosts are spread across the Malagasy *Pheidole* radiation. This provides an opportunity to test for selection on morphological similarity and divergence between parasites and hosts. Using X-ray microtomography and both linear measurements and three-dimensional (3D) geometric morphometrics, we show that ant social parasite worker morphologies feature a mix of "host-matching" and "parasitic" traits, where the former converge on the host phenotype and the latter diverge from typical *Pheidole* phenotypes to match a common parasitic syndrome. This finding highlights the role of social context in shaping the evolution of phenotypes and raises questions about the role of morphological sensing in nestmate recognition.

RESULTS AND DISCUSSION

Over the past two decades, intensive biodiversity inventories of the island of Madagascar have revealed a massive and highly endemic ant fauna, including around 100 putative species from the hyperdiverse genus *Pheidole* [10, 11]. We examined this material and observed that most ecological and morphological variants found in *Pheidole* around the globe are present in the Malagasy clade. Among this group, however, we found 13 unusual species, which we call the *Pheidole lucida* group (for the first of its two described species, *P. lucida*), all of which are associated with other *Pheidole* species in Madagascar (Data S1). Although the full biology of these species is not yet known, multiple lines of evidence suggest that they are inquilines (residing inside the nest of another species), and likely social parasites. First, they were frequently observed and collected as part of a nest series of other *Pheidole* species (i.e., the putative hosts). Second, they have a suite of morphological traits that are typically observed in other inquiline species. The minor worker caste has reduced mandibles and loss of cuticular pigmentation, whereas the queens show modifications found in many other inquiline species that are often referred to as part of a "parasitic syndrome" (e.g., rounded head shape, elongated antennae, broadened postpetiole, etc. [12, 13]). Third, the major worker subcaste, a hallmark of the genus and present in all 1,000+ non-parasitic *Pheidole* species, is entirely absent in the *P. lucida* group. In this genus, the partial loss of the worker caste is a strong indication of a socially parasitic lifestyle, where reproductive allocation to the worker caste is often reduced or lost entirely [6, 12–16]. Only one of the 13 inquiline species (*P.* gf010) seems to be entirely workerless, with the queen itself showing a very reduced, worker-like morphology. Sumner

Please cite this article in press as: Fischer et al., Socially Parasitic Ants Evolve a Mosaic of Host-Matching and Parasitic Morphological Traits, Current Biology (2020), https://doi.org/10.1016/j.cub.2020.06.078

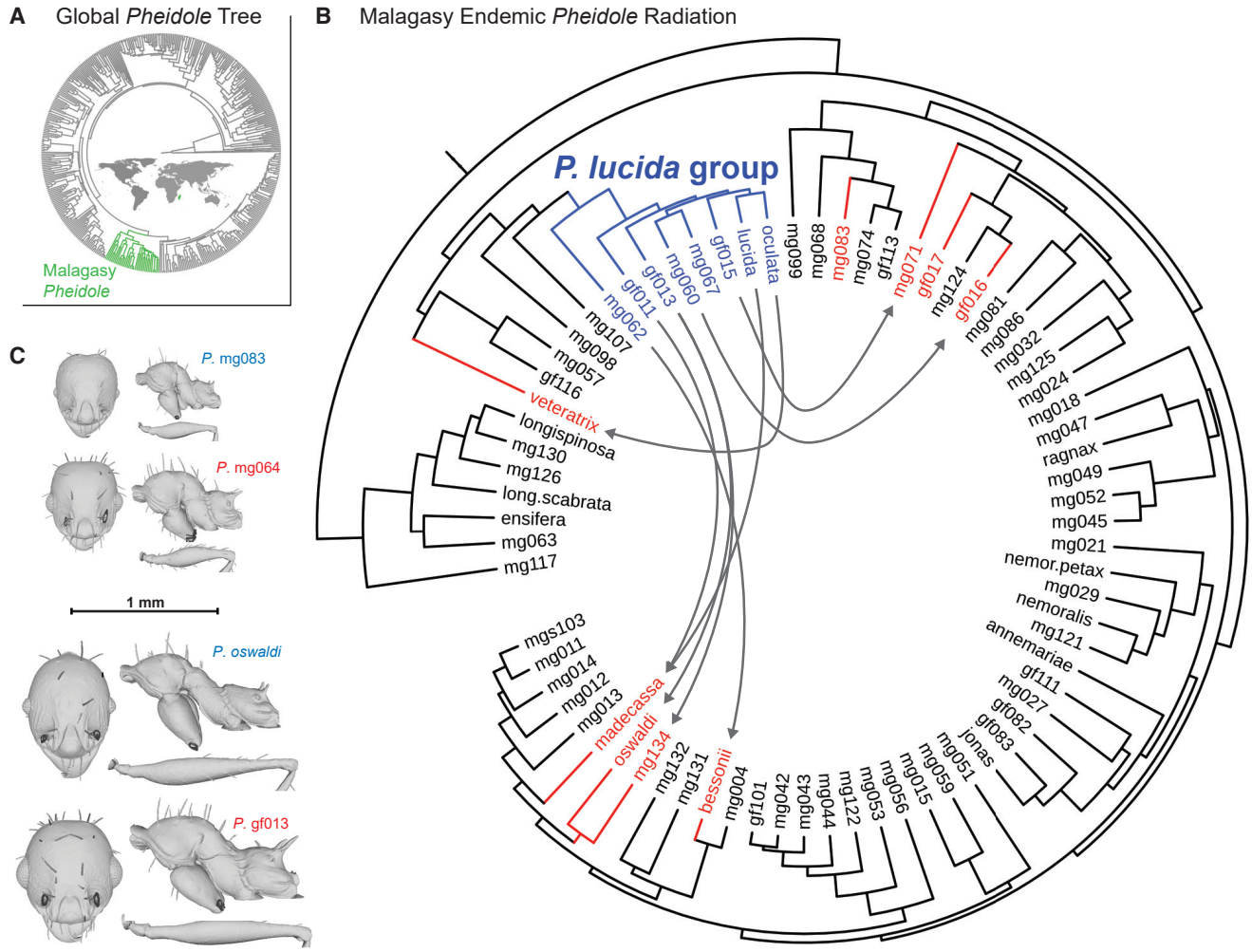

Figure 1. Evolution of Social Parasites within an Endemic Radiation of the Ant Genus *Pheidole* in Madagascar

(A) Nearly all Malagasy *Pheidole* species are part of a single endemic radiation (the tree was redrawn from [17]).

(B) Maximum-likelihood phylogeny of the Malagasy clade based on RAD-seq-derived DNA sequences and inferred with ExaML and dated with BEAST. The *P. lucida* group (blue) is a clade of social parasites that are associated with host species (red); arrows denote host-parasite pairs. Note that not all parasitic species and hosts are represented in the phylogeny (the tree was rendered with the interactive tree of life online tool; https://itol.embl.de). A larger specimen tree with node supports can be found in Figure S1A (specimen data are in Table S3).

(C) Comparison of smallest versus largest parasite-host pairs illustrates the host-matching pattern observed in Malagasy *Pheidole* social parasites (hosts in blue and parasites in red; for all species pairs, see Figure S1B) (see also Data S1 and Table S2).

et al. [16] suggested that workers of incipient social parasites (inquilines) may help the parasitic queen suppress host reproduction and redirect host resources toward the production of parasite queens and males. We refer to this group as "social parasites" because of the evidence above but, without direct observation, the strength of this parasitism in the *P. lucida* group is uncertain and we cannot rule out weak or even no costs to the host (i.e., commensalism). However, the important point for the following study is that if the workers in the *P. lucida* group are symbiotic with the host colonies, we should expect their phenotypes to be subject to scrutiny by the host workers in everyday social interactions.

A recent global-scale phylogeny of the genus [17] suggested that most *Pheidole* species in Madagascar are derived from a single colonization of the island (Figure 1A) and form a clade that is sister to the Australasian *Pheidole*. Using newly generated Restriction-site Associated DNA sequencing (RAD-seq) data, we reconstructed a new phylogeny with extensive sampling across Madagascar (75 out of ~100 species, including eight social parasites and all known hosts) and representative sampling of other Old World *Pheidole* groups. Our phylogenomic reconstruction (Figures 1B and S1) reconfirms previous findings [17] that almost all *Pheidole* in Madagascar are part of a single endemic radiation, with the remaining species being recent colonist lineages from the Afrotropical *Pheidole megacephala* group.

Whereas most previously known ant inquiline social parasites are closely related to their hosts (a phenomenon known as Emery's rule) [4–8], we found an unexpected pattern for the

Please cite this article in press as: Fischer et al., Socially Parasitic Ants Evolve a Mosaic of Host-Matching and Parasitic Morphological Traits, Current Biology (2020), https://doi.org/10.1016/j.cub.2020.06.078

Malagasy fauna: the parasitic *Pheidole* species in the phylogeny form a monophyletic group, with the hosts spread across the larger *Pheidole* radiation (Figures 1B and S1). This suggests social parasitism evolved in the ancestor of this clade, and parasite species subsequently radiated, infecting a range of different host species. Such an evolutionary scenario has not previously been documented for inquiline ant social parasites, although it has been observed in other forms of parasitism such as thievery and dulosis (brood parasitism or slave making [18, 19]).

Due to its monophyly, the socially parasitic *P. lucida* group constitutes a natural experiment that we can use to test selective pressures on ant species morphologies as they transition to different host species. We expect parasite traits to diverge from normal *Pheidole* morphologies, as has been observed in many other ant social parasites including *Pheidole* [12, 13]—but is there an evolutionary trend toward morphological similarity with the hosts in the *P. lucida* group? Qualitatively, body size and some other aspects of their morphologies appear to be correlated between host and parasite species, whereas other morphological aspects are disparate (Figures 1C, 2, 3, and S1B).

To investigate this quantitatively, we compared both linear measurements and three-dimensional (3D) geometric morphometric data (derived from X-ray micro-computed tomography [micro-CT] scan images) for workers of each host and social parasite species in a phylogenetic regression framework (phylogenetic generalized least squares; PGLS). We also employed a non-parametric permutation test by associating random pairs of parasites and non-host Malagasy *Pheidole* species and examining how often we recovered correlations.

As expected, we find evidence for distinct parasite-associated traits within the *P. lucida* group, in particular, significantly larger eyes and shorter mandibles in workers and a reduction of head and thorax proportions in the queen caste (Figures 2, S1, and S3). Procrustes analyses and principal-component (PC) axes describing morphological shape reveal these differences in fine detail. Not only do parasite species have shorter heads with larger eyes (Figure 3; head PC1, PC3) but their thorax morphology is more stocky and compactly built (mesosoma PC1, PC3, PC4). These characteristics may be associated with common features of inquiline life, or could be due to reduced selection on previously favored traits. In particular, reduced mandible size likely reflects less reliance on behaviors that require a robust set of mandibles, such as capturing and carrying prey [12, 20]. The advantage of the parasitic workers' larger eyes is unclear, but could reflect selection on a lifestyle confined within the dim, but not completely dark, environment of the nest and a possible necessity for visual nestmate recognition (because social parasites are chemically disguised).

In addition, we found a suite of traits that match between parasite and host workers. We first tested whether body sizes of hosts and parasites were correlated using linear measurements of different body parts. We found that measurements are highly correlated for thorax length (WL; Weber's length), as well as other features that scale with body size such as head length (HL) and head width (HW), indicating that overall body size of the parasites corresponds to that of their respective hosts (Figures 2 and S1B). In addition, measurements such as scape length (first antennal segment; SL) and femur length (of hind legs; FL; Figure 2A) of the parasites correspond strongly to those of their respective hosts. These relationships were confirmed in PGLS regressions (Figure 2B). To understand whether any shape correlation remained after correcting for allometric size-shape relationships, we performed multivariate PGLS regressions that included body size as covariate (Figure 2C); these showed that host-parasite similarity in SL and FL is independent of body size. We conducted a set of permutation tests with shuffled host-parasite pairs including 60 non-host Malagasy *Pheidole* species (Figure 2D), which showed that relationships between host and parasite traits always exceeded null expectations. Lastly, as an additional analysis intended to determine whether shape similarity was only driven by shared body size allometries, we constructed structured equation models (SEMs) including body size and shape trait values from both hosts and parasites (Figure S2). Overall, we observed that whereas parasite and host queens showed morphological divergence, their workers showed striking morphological similarities in size and shape (Figure 2E) unlikely to be due to chance alone.

Geometric morphometric analysis on landmarks placed on 3D surface models derived from CT scans showed marked similarity in thorax (mesosoma) shape between parasites and hosts (Figure 3). Parasites tended to exhibit a thicker, more rounded, compact head shape (head shape PC1, PC2, PC4) and a more robust, stockier thorax than their hosts (mesosoma shape PC1, PC4). Changes in thorax but not head characteristics were correlated between hosts and parasites (Figure 3B). Changes in thorax shape were also correlated with body size; however, a PGLS regression correcting for body size still found a significant relationship between the thorax shape of parasites and their hosts (Figure 3C). Likewise, head shape differed overall between hosts and parasites while still being correlated (Figure 3A), although this correlation was not significant after correcting for body size allometry (Figure 3C). Thus, some of the shape similarity between the parasites and their host species is likely attributable to body size correlation combined with common shape-size allometric scaling relationships. However, after correcting for such relationships, host-parasite correlations remained observable for several features of 3D body shape (head PC1, mesosoma PC1, PC3, PC4).

Worker surface sculpture and pigmentation do not consistently match between parasite and host species, and are often divergent in parasites. Whereas cuticles of host species range from smooth to fully punctate sculpture on the head and thorax and are yellow to dark brown in color, *P. lucida* group workers have a very smooth, translucent yellow to light orange cuticle (sculpture is present in only a few species, and in very small amounts). The latter is consistent with the parasitic syndrome and may be a result of reduced selection on these traits in the parasites. Worker standing hair density on head and anterior thorax dorsal surfaces, however, shows potential host matching (Figure 4). Although sample sizes for the statistical tests were low and the variability of this trait seems relatively high, a phylogenetically corrected PGLS analysis shows that the relative number of hairs per surface area is significantly correlated (Figure 4C) for parasite-host species pairs.

Because the parasitic queens have to accomplish invasion of the host nest and being accepted by the host workers, one might also expect the parasitic queens to match the morphology of the host queens. Yet, no evidence exists for morphological host

Please cite this article in press as: Fischer et al., Socially Parasitic Ants Evolve a Mosaic of Host-Matching and Parasitic Morphological Traits, Current Biology (2020), https://doi.org/10.1016/j.cub.2020.06.078

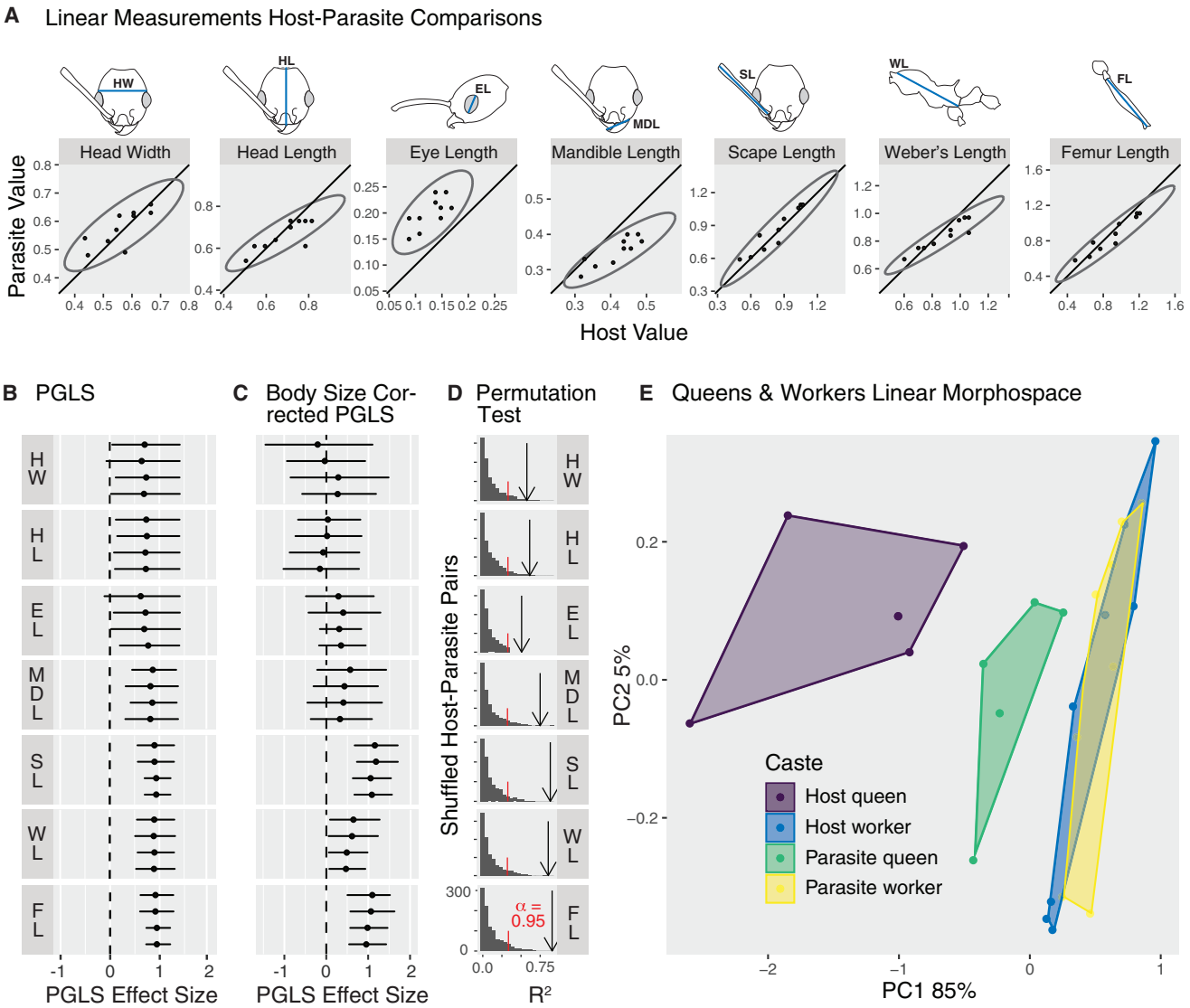

Figure 2. Two-Dimensional (2D) Morphospace of Malagasy *Pheidole* Parasite and Host Species

(A) Pairwise comparison of parasite versus host species linear measurements (see also Figures S2–S4, Data S1, and Table S1).

(B) Phylogenetic generalized least-squares (PGLS) regressions indicate that linear measurements show positive effect size and significant correlations between parasite and host species independent of phylogenetic relationships (character abbreviations are the same as in A; the different bars represent the four possible combinations of host phenotypes as predictor variables).

(C) Multivariate PGLS regressions including body size as a covariate show that at least femur and scape length (FL and SL) evolve independent of body size constraints (no allometry effect).

(D) Permutation test of shuffled host-parasite pairs, including 60 non-host *Pheidole* species, shows that host-parasite relationships always exceed null expectations (arrows denote the observed R^2 values).

(E) Host-parasite morphospace based on linear measurements shows clear separation of the worker versus the divergent host and parasite queen morphologies. PC1 represents differences in overall size and accounts for 85% of the variation, whereas differences in PC2 relate to individual body part sizes and proportions.

matching in parasitic queens. We measured all of the available parasite and host queens, resulting in six species pairs for comparison. Consistent with Wilson's parasitic syndrome [13], the parasitic queens are without exception smaller than the queens of their host (Figure S3), probably making it easier to infiltrate and persist in the colony undetected. Yet, although parasite queens are on average 35% smaller than their host queens, their body sizes are correlated (Figure S3A). This pattern could be driven by selection on parasitic worker size. However, the overall linear measurement morphospace (Figure 2E) clearly shows that parasitic queens cluster neither with host queens nor with host workers. Instead, they correlate more with the parasitic workers in overall size and a few other characteristics. The fact that parasitic queens' morphology does not evolve to match the host queen is somewhat enigmatic, given that there should be strong selection on hosts to identify and remove parasitic queens from

Please cite this article in press as: Fischer et al., Socially Parasitic Ants Evolve a Mosaic of Host-Matching and Parasitic Morphological Traits, Current Biology (2020), https://doi.org/10.1016/j.cub.2020.06.078

CellPress
OPEN ACCESS

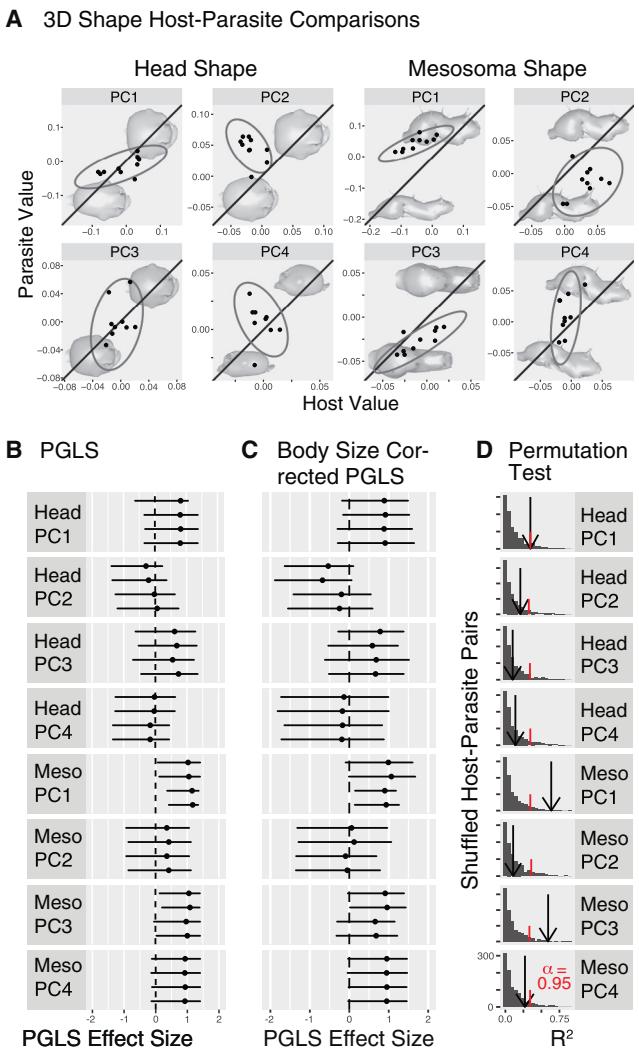

Figure 3. 3D Geometric Morphometric Procrustes Analyses

(A) 3D geometric morphometric shapes of parasites (y axis) converge with host species (x axis) in some dimensions such as head PC1 and PC3 and mesosoma (thorax) PC1, PC3, and PC4 (elongated versus short and compact shapes) but diverge, for example, in posterior head shape and eye size (head shape PC2) (see also Figures S2 and S4, Data S1, and Table S2).

(B–D) PGLS regressions show that these converging PC axes for head and mesosoma shape show significant positive correlations between parasites and host species (B; the different bars represent the four possible combinations of host phenotypes as predictor variables), even when using a correction coefficient for body size (C) and in permutation tests with shuffled host-parasite pairs (D) (arrows denote the observed R^2 values).

the nest. However, it is possible that systems for worker-worker recognition involve morphology whereas those for worker-queen recognition do not, perhaps due to the dominant influence of queen pheromones [21, 22].

In total, our results show evidence that the shapes and sizes of parasite workers match the host workers to some degree, even as hosts and parasites are not each other's closest relatives (as in Emery's rule [4–8]). Moreover, although shape allometry combined with body size correlation can explain some of the shape correlation, substantial additional shape correlation remains unexplained by body size allometry. Across the ant body, there are some traits that are divergent in all parasitic species, whereas others match the host. This implies that, whereas some traits evolve to suit a parasitic lifestyle (e.g., transparent [callow] cuticle, reduced mandibles, almost absent surface sculpture, and larger eyes), others evolve to match the host (overall body size, thorax shape, and relative leg and antennal lengths). As a result, the parasite phenotype is a mosaic of these traits.

In our view, the most straightforward explanation for this evolutionary pattern is that ants use morphological traits in concert with colony odor for nestmate recognition, so parasitic ant workers must adapt their morphology to blend in with the colony. Parasites often evolve remarkable adaptations to evade defense mechanisms of their hosts, and these adaptations are often as revealing about the biology of the host as they are about the parasite [2, 23–27]. Social parasites exploit the mechanisms of social organisms, often defeating social recognition systems to reap the benefits of cooperation without contributing in return [12]. Ant colonies are an attractive target for social parasites, as ants are among the most abundant terrestrial animals on Earth, and their colonies have been exploited by a wide range of parasitic organisms from beetles and butterflies to flies [1, 26, 28, 29], as well as other ant species [6, 14].

Many social parasites of ant colonies are known to mimic different aspects of the host's phenotype. Social parasites that are integrated into the ant society (i.e., inquilines) typically mimic or adopt the host's cuticular hydrocarbon profile [30–34], a primary tool for nestmate recognition in ants [35–38], yet not an exclusive one [39, 40]. Some non-ant inquilines have evolved further deceptions, such as behavioral and acoustic mimicry, in order to avoid host defenses [25, 27, 41–43]. Morphological mimicry has been documented among non-ant social parasites of ants [1, 2, 14, 26, 44, 45]. Many of these cases of morphological mimicry most likely evolved as a means to evade predators by blending in with ants outside the nest (i.e., Batesian mimicry). E. Wasmann (e.g., [3, 46]) documented a phenomenon where colony-integrated myrmecophiles resemble the morphology of their ant hosts in an apparent attempt to fool the host rather than a predator, later named Wasmannian mimicry [47]. Some systems, for example, the striking morphological convergence of myrmecophilous rove beetles with their army ant hosts, are thought to result from a combination of Batesian and Wasmannian mimicry. In the case of the rove beetles, their morphological mimicry has been suggested to both evade predators during swarm raids or in the nomadic phase (Batesian mechanism) and to help avoid detection in the colony by host ants through tactile mimicry [3, 26, 48]. Evidence for the latter can be found in the fact that some of the parasitic beetles mimic the surface texture of different host body parts [2, 26] and that parasites of subterranean army ants (lacking visual predators) mimic host morphology but not color. Similarly, ant parasites that attach directly to the ant body mimic the microcuticular structure and pilosity of the body part that they attach to or cover [40, 49], a fact consistent with a Wasmannian mechanism intended to fool the ant rather than a Batesian mechanism to discourage predators.

Why has the phenomenon of morphological matching not been observed previously for socially parasitic ants? There are

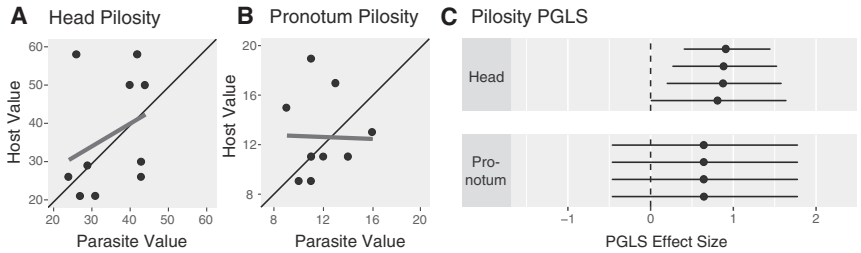

Figure 4. Head and Thorax Pilosity

(A and B) Pairwise comparison for host versus parasite head pilosity (A), but not anterior thorax (promesonotum) pilosity (B), shows a correlation in the number of standing hairs (linear regression line in grey; see also Data S1).

(C) PGLS regressions show a statistically significant correlation between parasite and host pairs (the different bars represent the four possible combinations of host phenotypes as predictor variables).

several potential explanations. First, organisms as different as rove beetles may need to evolve to be "ant-like" in order to avoid detection, but inquiline ants could already be morphologically similar enough without further modification. Or, there may be selection on morphological similarity even among ants, but because most inquiline ant species are closely related to their hosts (i.e., due to Emery's rule), they are expected to have correlated morphology due to shared ancestry, making any selection on similarity difficult to detect. Our analysis of the unusual evolutionary scenario of the socially parasitic *P. lucida* group radiation in Madagascar supports the latter explanation for this gap in the literature.

We concede that we can only speculate on the mechanism behind this pattern at this stage, as social parasites are difficult to study experimentally, and these Malagasy species are particularly remote and rare. There are at least two alternative hypotheses for this pattern that would not require mimicry as a mechanism—although, in our opinion, these would be equally interesting. First, if environmental factors during development (e.g., social care, diet/nutrition, or microbiome, etc.) have a strong and phylogenetically conserved effect on *Pheidole* size and shape, it is possible that interspecific individuals reared in the same nest could develop similar phenotypes during ontogeny—without any underlying changes on the genetic level. We know of no evidence of such an interspecific effect in ants and, although we consider this to be less likely than natural selection on morphology, we cannot rule out the possibility of such a fascinating scenario without further data. Second, it is possible that natural selection on existence in the physical nest environment (for example, tunnel size) could lead to selection on common morphological traits. Such a strong effect of nest environment on morphology is unknown in ants, and this would require that the nest environment has stronger selection pressure than the ecology of the hosts outside the nest (because hosts but not parasites forage). Although we cannot rule this out, this strikes us as less likely because the nest already accommodates very divergent body sizes and shapes, i.e., for minor and major workers as well as males and queens, so it is unclear how this would result in such tight constraints on minor worker morphology. Further work is needed to examine the mechanisms underlying this pattern.

In his foundational work on mimicry in ant host-parasite systems, Wasmann wrote that in addition to chemical (odor) deception, social parasites also need to exhibit morphological features that the host workers recognize as their own, what Wasmann called "Tast-Mimikry" (tactile mimicry [46]). Our finding that the morphology of social parasite ants gets tuned to the size and shape of their hosts suggests these discriminatory abilities may be very refined in ants. This raises the more general question of the role of morphological sensing in social insect recognition systems, a topic that has remained understudied as the field has focused on chemosensory mechanisms [37, 38, 50].

STAR★METHODS

Detailed methods are provided in the online version of this paper and include the following:

- KEY RESOURCES TABLE
- RESOURCE AVAILABILITY
  - Lead Contact
  - Materials Availability
  - Data and Code Availability
- EXPERIMENTAL MODEL AND SUBJECT DETAILS
- METHOD DETAILS
  - Material studied
  - DNA extraction and sequencing
- QUANTIFICATION AND STATISTICAL ANALYSIS
  - *de novo* assembly of RAD loci
  - Phylogenomic reconstruction
  - Linear measurements (2D morphology)
  - X-ray micro-CT scanning and 3D geometric landmarks (3D morphology)
  - Comparative Analysis
- ADDITIONAL RESOURCES

SUPPLEMENTAL INFORMATION

Supplemental Information can be found online at https://doi.org/10.1016/j.cub.2020.06.078.

ACKNOWLEDGMENTS

For fieldwork conducted in Madagascar, permits to research, collect, and export ants were obtained from the Ministry of Environment and Forest as part of an ongoing collaboration between the California Academy of Sciences and the Ministry of Environment and Forest, Madagascar National Parks, and Parc Botanique et Zoologique de Tsimbazaza. Authorization for export was provided by the director of natural resources. The fieldwork on which this study is based could not have been completed without the gracious support of the Malagasy people and the Arthropod Inventory Team (Balsama Rajemison, Jean-Claude Rakotonirina, Jean-Jacques Rafanomezantsoa, Chrislain Ranaivo, Hanitriniana Rasoazanamavo, Nicole Rasoamanana, Clavier Randrianandrasana, Dimby Raharinjanahary, Njaka Ravelomanana, Manoa Ramamonjisoa, Mihary Razafimamonjy, Pascal Rabeson, and Emile Rajeriarison). All fieldwork was funded by National Science Foundation grants DEB-0072713, DEB-0344731, and DEB-0842395 (to B.L.F.). Lab work was supported by a National Science Foundation grant (DEB-1145989) (to E.P.E. and L.L.K.) and subsidy funding to OIST. Specimen images on AntWeb were

taken by Michele Esposito for which we are very grateful. Loaned type and non-type material was kindly provided by Dr. Bernard Landry (MHNG) and Dr. Gary Alpert (MCZC). We also thank Jo Ann Tan for laboratory work related to sequencing, and Miguel Grau Lopez for help with bioinformatics. We thank the OIST DNA Sequencing Section, Imaging Section, and Scientific Computing Section for assistance conducting this research. This work was supported by subsidy funding to OIST, and a JSPS KAKENHI grant-in-aid (to E.P.E.) (17K15180).

AUTHOR CONTRIBUTIONS

Conceived and designed the study; G.F., E.P.E., and B.L.F. Collected the specimens; B.L.F. Performed specimen work and identifications; G.F. and B.L.F. Molecular work was performed in A.S.M.'s laboratory. Performed micro-CT; G.F. Analyzed the data; G.F., N.R.F., N.N., L.L.K., A.S.M., and E.P.E. Contributed reagents/materials/analysis tools; J.-P.H., L.L.K., N.N., and A.S.M. Wrote the paper; G.F., N.R.F., and E.P.E., with contributions from all co-authors.

DECLARATION OF INTERESTS

The authors declare no competing interests.

Received: June 19, 2019
Revised: March 18, 2020
Accepted: June 23, 2020
Published: July 23, 2020

REFERENCES

1. McIver, J.D., and Stonedahl, G. (1993). Myrmecomorphy: morphological and behavioral mimicry of ants. Annu. Rev. Entomol. *38*, 351–377.
2. Maruyama, M., and Parker, J. (2017). Deep-time convergence in rove beetle symbionts of army ants. Curr. Biol. *27*, 920–926.
3. Wasmann, E. (1895). Die Ameisen- und Termitengäste von Brasilien. I. Theil. Mit einem Anhange von Dr. August Forel. Verh. K. K. Zool.-Bot. Ges. Wien *45*, 137–179.
4. Emery, C. (1909). Über den Ursprung der dulotischen, parasitischen und myrekophilen Ameisen. Biol. Zentralbl. *29*, 352–362.
5. Bourke, A.F., and Franks, N.R. (1991). Alternative adaptations, sympatric speciation and the evolution of parasitic, inquiline ants. Biol. J. Linn. Soc. Lond. *43*, 157–178.
6. Buschinger, A. (2009). Social parasitism among ants: a review (Hymenoptera: Formicidae). Myrmecol. News *12*, 219–235.
7. Jansen, G., Savolainen, R., and Vepsäläinen, K. (2010). Phylogeny, divergence-time estimation, biogeography and social parasite-host relationships of the Holarctic ant genus *Myrmica* (Hymenoptera: Formicidae). Mol. Phylogenet. Evol. *56*, 294–304.
8. Rabeling, C., Schultz, T.R., Pierce, N.E., and Bacci, M., Jr. (2014). A social parasite evolved reproductive isolation from its fungus-growing ant host in sympatry. Curr. Biol. *24*, 2047–2052.
9. Nash, D.R., and Boomsma, J.J. (2008). Communication between hosts and social parasites. In Sociobiology of Communication: An Interdisciplinary Perspective, P. d'Ettorre, and D.P. Hughes, eds. (Oxford University Press), pp. 55–79.
10. Fisher, B.L., and Peeters, C. (2019). Ants of Madagascar: A Guide to the 62 Genera (Association Vahatra).
11. Fischer, G., and Fisher, B.L. (2013). A revision of *Pheidole* Westwood (Hymenoptera: Formicidae) in the islands of the southwest Indian Ocean and designation of a neotype for the invasive *Pheidole megacephala*. Zootaxa *3683*, 301–356.
12. Wilson, E.O. (1971). The Insect Societies (Harvard University Press).
13. Wilson, E.O. (1984). Tropical social parasites in the ant genus *Pheidole*, with an analysis of the anatomical parasitic syndrome (Hymenoptera: Formicidae). Insectes Soc. *31*, 316–334.
14. Hölldobler, B., and Wilson, E.O. (1990). The Ants (Harvard University Press).
15. Maschwitz, U., Dorow, W., Buschinger, A., and Kalytta, G. (2000). Social parasitism involving ants of different subfamilies: *Polyrhachis lama* (Formicinae) an obligatory inquiline of *Diacamma* sp. (Ponerinae) in Java. Insectes Soc. *47*, 27–35.
16. Sumner, S., Nash, D.R., and Boomsma, J.J. (2003). The adaptive significance of inquiline parasite workers. Proc. Biol. Sci. *270*, 1315–1322.
17. Economo, E.P., Huang, J.P., Fischer, G., Sarnat, E.M., Narula, N., Janda, M., Guénard, B., Longino, J.T., and Knowles, L.L. (2019). Evolution of the latitudinal diversity gradient in the hyperdiverse ant genus *Pheidole*. Glob. Ecol. Biogeogr. *28*, 456–470.
18. Beibl, J., Buschinger, A., Foitzik, S., and Heinze, J. (2007). Phylogeny and phylogeography of the Mediterranean species of the parasitic ant genus *Chalepoxenus* and its *Temnothorax* hosts. Insectes Soc. *54*, 189–199.
[19]. Adams, R.M.M. (2008). Unraveling the origins of social parasitism in *Megalomyrmex* ants. PhD dissertation (The University of Texas at Austin).
20. Wilson, E.O., and Brown, W.L. (1956). New parasitic ants of the genus *Kyidris*, with notes on ecology and behavior. Insectes Soc. *3*, 439–454.
21. Van Oystaeyen, A., Oliveira, R.C., Holman, L., van Zweden, J.S., Romero, C., Oi, C.A., d'Ettorre, P., Khalesi, M., Billen, J., Wäckers, F., et al. (2014). Conserved class of queen pheromones stops social insect workers from reproducing. Science *343*, 287–290.
22. Holman, L., Hanley, B., and Millar, J.G. (2016). Highly specific responses to queen pheromone in three *Lasius* ant species. Behav. Ecol. Sociobiol. *70*, 387–392.
23. Savolainen, R., and Vepsäläinen, K. (2003). Sympatric speciation through intraspecific social parasitism. Proc. Natl. Acad. Sci. USA *100*, 7169–7174.
24. Jones, C.B. (2005). Social parasitism in mammals with particular reference to Neotropical primates. Mastozool. Neotrop. *12*, 19–35.
25. Barbero, F., Thomas, J.A., Bonelli, S., Balletto, E., and Schönrogge, K. (2009). Queen ants make distinctive sounds that are mimicked by a butterfly social parasite. Science *323*, 782–785.
26. Parker, J. (2016). Myrmecophily in beetles (Coleoptera): evolutionary patterns and biological mechanisms. Myrmecol. News *22*, 65–108.
27. Di Giulio, A., Maurizi, E., Barbero, F., Sala, M., Fattorini, S., Balletto, E., and Bonelli, S. (2015). The pied piper: a parasitic beetle's melodies modulate ant behaviours. PLoS ONE *10*, e0130541.
28. Wasmann, E. (1894). Kritisches Verzeichniss der myrmekophilen und termitophilen Arthropoden: Mit Angabe der Lebensweise und mit Beschreibung neuer Arten (FL Dames).
29. Witek, M., Barbero, F., and Markó, B. (2014). *Myrmica* ants host highly diverse parasitic communities: from social parasites to microbes. Insectes Soc. *61*, 307–323.
30. Lenoir, A., D'Ettorre, P., Errard, C., and Hefetz, A. (2001). Chemical ecology and social parasitism in ants. Annu. Rev. Entomol. *46*, 573–599.
31. D'Ettorre, P., Mondy, N., Lenoir, A., and Errard, C. (2002). Blending in with the crowd: social parasites integrate into their host colonies using a flexible chemical signature. Proc. Biol. Sci. *269*, 1911–1918.
32. Howard, R.W., and Blomquist, G.J. (2005). Ecological, behavioral, and biochemical aspects of insect hydrocarbons. Annu. Rev. Entomol. *50*, 371–393.
33. Akino, T. (2008). Chemical strategies to deal with ants: a review of mimicry, camouflage, propaganda, and phytomimesis by ants (Hymenoptera: Formicidae) and other arthropods. Myrmecol. News *11*, 173–181.
34. Uboni, A., Bagnères, A.-G., Christidès, J.-P., and Lorenzi, M.C. (2012). Cleptoparasites, social parasites and a common host: chemical insignificance for visiting host nests, chemical mimicry for living in. J. Insect Physiol. *58*, 1259–1264.
35. Dettner, K., and Liepert, C. (1994). Chemical mimicry and camouflage. Annu. Rev. Entomol. *39*, 129–154.

36. Brandt, M., Foitzik, S., Fischer-Blass, B., and Heinze, J. (2005). The coevolutionary dynamics of obligate ant social parasite systems—between prudence and antagonism. Biol. Rev. Camb. Philos. Soc. *80*, 251–267.

37. Sturgis, S.J., and Gordon, D.M. (2012). Nestmate recognition in ants (Hymenoptera: Formicidae): a review. Myrmecol. News *16*, 101–110.

38. Sprenger, P.P., and Menzel, F. (2020). Cuticular hydrocarbons in ants (Hymenoptera: Formicidae) and other insects: how and why they differ among individuals, colonies, and species. Myrmecol. News *30*, 1–26.

39. von Beeren, C., Hashim, R., and Witte, V. (2012). The social integration of a myrmecophilous spider does not depend exclusively on chemical mimicry. J. Chem. Ecol. *38*, 262–271.

40. von Beeren, C., and Tishechkin, A.K. (2017). *Nymphister kronaueri* von Beeren & Tishechkin sp. nov., an army ant-associated beetle species (Coleoptera: Histeridae: Haeteriinae) with an exceptional mechanism of phoresy. BMC Zool. *2*, 3.

41. Schönrogge, K., Barbero, F., Casacci, L., Settele, J., and Thomas, J. (2017). Acoustic communication within ant societies and its mimicry by mutualistic and socially parasitic myrmecophiles. Anim. Behav. *134*, 249–256.

42. Hölldobler, K. (1953). Gibt es in Deutschland Ameisengäste, die echte Täuscher sind? Naturwissenschaften *40*, 34–35.

43. Maurizi, E., Fattorini, S., Moore, W., and Di Giulio, A. (2012). Behavior of *Paussus favieri* (Coleoptera, Carabidae, Paussini): a myrmecophilous beetle associated with *Pheidole pallidula* (Hymenoptera, Formicidae). Psyche *2012*, 940315.

44. Hölldobler, B. (1971). Communication between ants and their guests. Sci. Am. *224*, 86–95.

45. Pérez-Espona, S., Goodall-Copestake, W., Berghoff, S., Edwards, K., and Franks, N. (2018). Army imposters: diversification of army ant-mimicking beetles with their *Eciton* hosts. Insectes Soc. *65*, 59–75.

46. Wasmann, E., and Aachen, S.J. (1925). Die Ameisenmimikry. Naturwissenschaften *13*, 944–951.

47. Rettenmeyer, C.W. (1970). Insect mimicry. Annu. Rev. Entomol. *15*, 43–74.

48. von Beeren, C., Brückner, A., Maruyama, M., Burke, G., Wieschollek, J., and Kronauer, D.J.C. (2018). Chemical and behavioral integration of army ant-associated rove beetles—a comparison between specialists and generalists. Front. Zool. *15*, 8.

49. Kistner, D.H. (1979). Social and evolutionary significance of social insect symbionts. In Social Insects, *vol. 1*, H.R. Hermann, ed. (Academic Press), pp. 339–413.

50. Bos, N., and d'Ettorre, P. (2012). Recognition of social identity in ants. Front. Psychol. *3*, 83.

51. Eaton, D., and Overcast, I. (2017). ipyrad: interactive assembly and analysis of RADseq data sets.. http://ipyrad.readthedocs.io.

52. Stamatakis, A. (2014). RAxML version 8: a tool for phylogenetic analysis and post-analysis of large phylogenies. Bioinformatics *30*, 1312–1313.

53. Kozlov, A.M., Aberer, A.J., and Stamatakis, A. (2015). ExaML version 3: a tool for phylogenomic analyses on supercomputers. Bioinformatics *31*, 2577–2579.

54. Bouckaert, R., Vaughan, T.G., Barido-Sottani, J., Duchêne, S., Fourment, M., Gavryushkina, A., Heled, J., Jones, G., Kühnert, D., De Maio, N., et al. (2019). BEAST 2.5: an advanced software platform for Bayesian evolutionary analysis. PLoS Comput. Biol. *15*, e1006650.

55. Lanfear, R., Frandsen, P.B., Wright, A.M., Senfeld, T., and Calcott, B. (2017). PartitionFinder 2: new methods for selecting partitioned models of evolution for molecular and morphological phylogenetic analyses. Mol. Biol. Evol. *34*, 772–773.

56. Bolger, A.M., Lohse, M., and Usadel, B. (2014). Trimmomatic: a flexible trimmer for Illumina sequence data. Bioinformatics *30*, 2114–2120.

57. Cignoni, P., Callieri, M., Corsini, M., Dellepiane, M., Ganovelli, F., and Ranzuglia, G. (2008). Meshlab: an open-source mesh processing tool. In Eurographics Italian Chapter Conference, *vol. 2008*, V. Scarano, R. De Chiara, and U. Erra, eds. , pp. 129–136.

58. Stratovan Corporation (2019). Stratovan Checkpoint, version 2019.03.04.1102. https://www.stratovan.com/products/checkpoint.

59. Pennell, M.W., Eastman, J.M., Slater, G.J., Brown, J.W., Uyeda, J.C., FitzJohn, R.G., Alfaro, M.E., and Harmon, L.J. (2014). Geiger v2.0: an expanded suite of methods for fitting macroevolutionary models to phylogenetic trees. Bioinformatics *30*, 2216–2218.

60. Pinheiro, J., Bates, D., DebRoy, S., and Sarkar, D.; R Core Team (2019). nlme: linear and nonlinear mixed effects models. R package, version 3.1-141.

61. Adams, D.C., and Otárola-Castillo, E. (2013). geomorph: an R package for the collection and analysis of geometric morphometric shape data. Methods Ecol. Evol. *4*, 393–399.

62. Rosseel, Y. (2012). Lavaan: an R package for structural equation modeling and more. Version 0.5-12 (BETA). J. Stat. Softw. *48*, 1–36.

[63]. Revell, L.J. (2012). phytools: An R package for phylogenetic comparative biology (and other things). Method in Ecology and Evolution*3* (British Ecological Society), pp. 217–223.

64. Rambaout, A. (2012). FigTree, version 1.4. http://tree.bio.ed.ac.uk/software/figtree/.

65. Letunic, I., and Bork, P. (2019). Interactive tree of life (iTOL) v4: recent updates and new developments. Nucleic Acids Res. *47*, W256–W259.

66. Baird, N.A., Etter, P.D., Atwood, T.S., Currey, M.C., Shiver, A.L., Lewis, Z.A., Selker, E.U., Cresko, W.A., and Johnson, E.A. (2008). Rapid SNP discovery and genetic mapping using sequenced RAD markers. PLoS ONE *3*, e3376.

67. Tin, M.M.-Y., Economo, E.P., and Mikheyev, A.S. (2014). Sequencing degraded DNA from non-destructively sampled museum specimens for RAD-tagging and low-coverage shotgun phylogenetics. PLoS ONE *9*, e96793.

68. Tin, M.M.-Y., Rheindt, F.E., Cros, E., and Mikheyev, A.S. (2015). Degenerate adaptor sequences for detecting PCR duplicates in reduced representation sequencing data improve genotype calling accuracy. Mol. Ecol. Resour. *15*, 329–336.

69. Eaton, D.A.R., Spriggs, E.L., Park, B., and Donoghue, M.J. (2017). Misconceptions on missing data in RAD-seq phylogenetics with a deep-scale example from flowering plants. Syst. Biol. *66*, 399–412.

70. Chifman, J., and Kubatko, L. (2014). Quartet inference from SNP data under the coalescent model. Bioinformatics *30*, 3317–3324.

71. Fischer, G., Sarnat, E.M., and Economo, E.P. (2016). Revision and microtomography of the *Pheidole knowlesi* group, an endemic ant radiation in Fiji (Hymenoptera, Formicidae, Myrmicinae). PLoS ONE *11*, e0158544.

72. Sarnat, E.M., Fischer, G., and Economo, E.P. (2016). Inordinate spinescence: taxonomic revision and microtomography of the *Pheidole cervicornis* species group (Hymenoptera, Formicidae). PLoS ONE *11*, e0156709.

73. Hita Garcia, F., Fischer, G., Liu, C., Audisio, T.L., Alpert, G.D., Fisher, B.L., and Economo, E.P. (2017). X-ray microtomography for ant taxonomy: an exploration and case study with two new *Terataner* (Hymenoptera, Formicidae, Myrmicinae) species from Madagascar. PLoS ONE *12*, e0172641.

74. Zelditch, M.L., Swiderski, D.L., and Sheets, H.D. (2012). Geometric Morphometrics for Biologists: A Primer (Academic Press).

75. Cooney, C.R., Bright, J.A., Capp, E.J.R., Chira, A.M., Hughes, E.C., Moody, C.J.A., Nouri, L.O., Varley, Z.K., and Thomas, G.H. (2017). Mega-evolutionary dynamics of the adaptive radiation of birds. Nature *542*, 344–347.

76. Pagel, M. (1999). Inferring the historical patterns of biological evolution. Nature *401*, 877–884.

Please cite this article in press as: Fischer et al., Socially Parasitic Ants Evolve a Mosaic of Host-Matching and Parasitic Morphological Traits, Current Biology (2020), https://doi.org/10.1016/j.cub.2020.06.078

STAR★METHODS

KEY RESOURCES TABLE

REAGENT or RESOURCE	SOURCE	IDENTIFIER
Deposited Data		
RAD-seq DNA sequences	DDBJ (Digital Data Bank of Japan)	Project ID: PRJDB9763
X-ray micro-CT generated surfaces of workers	Datadryad	https://datadryad.org/stash/share/oQZatOFkkBXcsaQGs1mc-hxTuls64YQYWFS3YfzAiKI
Linear measurements of workers	Datadryad	https://datadryad.org/stash/share/oQZatOFkkBXcsaQGs1mc-hxTuls64YQYWFS3YfzAiKI
Geometric morphometric landmark files	Datadryad	https://datadryad.org/stash/share/oQZatOFkkBXcsaQGs1mc-hxTuls64YQYWFS3YfzAiKI
DNA sequence alignment	Datadryad	https://datadryad.org/stash/share/oQZatOFkkBXcsaQGs1mc-hxTuls64YQYWFS3YfzAiKI
Lab Equipment		
Illumina HiSeq 2500		https://www.illumina.com
Leica M12.5 dissecting microscope	Leica Microsystems	https://www.leica-microsystems.com/
Leica M165C dissecting microscope	Leica Microsystems	https://www.leica-microsystems.com/
100 line orthogonal crosshair micrometer	Leica Microsystems	https://www.leica-microsystems.com/
ZEISS Xradia 510 Versa micro-CT scanner	Zeiss Microscopy	https://www.zeiss.com/microscopy/int/products/x-ray-microscopy.html
Software and Algorithms		
ipyrad v0.7.13	[51]	https://ipyrad.readthedocs.io/en/latest/index.html
RaxML v8.2.4c	[52]	https://cme.h-its.org/exelixis/web/software/raxml/
ExaML v3.0.17	[53]	https://cme.h-its.org/exelixis/web/software/examl/index.html
BEAST v2.4.8	[54]	https://www.beast2.org/
partitionfinder v2.1.1	[55]	http://www.robertlanfear.com/partitionfinder/
Trimmomatic	[56]	http://www.usadellab.org/cms/?page=trimmomatic
ZEISS Scout and Scan Control Software	Zeiss Microscopy	https://www.zeiss.com/microscopy/int/products/x-ray-microscopy.html
Amira v6.5	Thermo Fisher Scientific	https://www.thermofisher.com
Meshlab v2016.12	[57]	http://www.meshlab.net/
Stratovan Checkpoint version 2018.08.07	[58]	https://www.stratovan.com/products/checkpoint
R version 3.5.2	The R Project for Statistical Computing	https://www.r-project.org/
R package *geiger* version 2.0.6.1	[59]	https://cran.r-project.org/web/packages/geiger/index.html
R package *nlme* version 3.1-137	[60]	https://cran.r-project.org/web/packages/nlme/index.html
R package *geomorph* version 3.0.7	[61]	https://cran.r-project.org/web/packages/geomorph/index.html
R package *lavaan* version 0.6-3	[62]	https://cran.r-project.org/web/packages/lavaan/index.html
R package *phytools* version 0.6-60	[63]	https://cran.r-project.org/web/packages/phytools/index.html
FigTree v1.4	[64]	http://tree.bio.ed.ac.uk/software/figtree/
iTOL v4	[65]	https://itol.embl.de/

Please cite this article in press as: Fischer et al., Socially Parasitic Ants Evolve a Mosaic of Host-Matching and Parasitic Morphological Traits, Current Biology (2020), https://doi.org/10.1016/j.cub.2020.06.078

RESOURCE AVAILABILITY

Lead Contact

Further information and requests for resources should be directed to the Lead Contact, Georg Fischer (georgf81@gmail.com).

Materials Availability

This study did not generate new unique reagents.

Data and Code Availability

The datasets generated during this study are available at Datadryad [accession code/web link – https://datadryad.org/stash/share/oQZatOFkkBXcsaQGs1mc-hxTuIs64YQYWFS3YfzAiKI].

EXPERIMENTAL MODEL AND SUBJECT DETAILS

The following ant (Hymenoptera: Formicidae) species were used in this study: Pheidole afr001, Pheidole annemariae, Pheidole bessonii, Pheidole colaensis, Pheidole decepticon, Pheidole dodo, Pheidole ensifera, Pheidole fervens, Pheidole gf011, Pheidole gf012, Pheidole gf013, Pheidole gf015, Pheidole gf016, Pheidole gf017, Pheidole gf074, Pheidole gf075, Pheidole gf082, Pheidole gf083, Pheidole gf092, Pheidole gf093, Pheidole gf094, Pheidole gf095, Pheidole gf098, Pheidole gf101, Pheidole gf111, Pheidole gf113, Pheidole gf116, Pheidole grallatrix, Pheidole indica, Pheidole jonas, Pheidole knowlesi, Pheidole longispinosa, Pheidole longispinosa scabrata, Pheidole lucida, Pheidole madecassa, Pheidole manteroi, Pheidole megacephala, Pheidole megacephala melancholica, Pheidole megacephala rotundata, Pheidole megacephala spinosa, Pheidole megacephala talpa, Pheidole megatron, Pheidole mg004, Pheidole mg011, Pheidole mg012, Pheidole mg013, Pheidole mg014, Pheidole mg015, Pheidole mg018, Pheidole mg021, Pheidole mg024, Pheidole mg027, Pheidole mg029, Pheidole mg032, Pheidole mg042, Pheidole mg043, Pheidole mg044, Pheidole mg045, Pheidole mg047, Pheidole mg049, Pheidole mg051, Pheidole mg052, Pheidole mg053, Pheidole mg 054, Pheidole mg056, Pheidole mg057, Pheidole mg059, Pheidole mg060, Pheidole mg062, Pheidole mg063, Pheidole mg064, Pheidole mg065, Pheidole mg067, Pheidole mg068, Pheidole mg071, Pheidole mg074, Pheidole mg081, Pheidole mg083, Pheidole mg086, Pheidole mg098, Pheidole mg099, Pheidole mg107, Pheidole mg117, Pheidole mg121, Pheidole mg122, Pheidole mg124, Pheidole mg125, Pheidole mg126, Pheidole mg130, Pheidole mg131, Pheidole mg132, Pheidole mg134, Pheidole mgs103, Pheidole nemoralis, Pheidole nemoralis petax, Pheidole oceanica, Pheidole oculata, Pheidole onifera, Pheidole oswaldi, Pheidole punctulata, Pheidole ragnax, Pheidole roberti, Pheidole SA02, Pheidole sikorae, Pheidole squalida, Pheidole ululevu, Pheidole umbonata, Pheidole veteratrix.

METHOD DETAILS

Material studied

Most of the material used for this study originates from inventory samples collected in the Malagasy region between 1992 and 2012 by Brian L. Fisher and the Malagasy Arthropod Team. Additional specimens were collected and loaned to the first author by Dr. Gary Alpert (MCZ). Morphological characterizations of the focal species in this study were performed for a taxonomic revision currently in preparation that includes the described and undescribed *P. lucida* group species and their hosts (Fischer et al. in prep). The taxonomic methodology adheres to myrmecological standards and includes close scrutiny of the available material in the collections of the California Academy of Sciences (CAS) and the Harvard Museum of Comparative Zoology (MCZ) entomology collections, as well as type material of already described species studied at and loaned from the Natural History Museum of Geneva (MHNG). For species delimitation purposes, linear measurements (Table S1) and 3D X-ray micro-CT scans (Table S2) were done for representatives of each treated species. Species morphology comparisons were done in two ways; the first is based on traditional linear measurements commonly used in ant literature, and the second on 3D geometric-morphometric landmarks. Compound light microscope images of all species and morphospecies are available at AntWeb (https://www.antweb.org).

DNA extraction and sequencing

We used a RAD-seq [66] pipeline to generate a molecular dataset to reconstruct a new phylogeny of Malagasy *Pheidole* (specimen metadata in Table S3). The RAD-seq method obtains large amounts of informative data at relatively low cost, and can handle degraded DNA which is common in field collections and museum samples such as those used in this project. We first extracted genomic DNA from each specimen using a non-destructive method by soaking overnight in a chaotropic buffer [67], then digested the DNA with the restriction enzyme EcoRI. We followed a semi-automated RAD library preparation protocol [68] based on the Biomek® FXP Laboratory Automation Workstation (Beckman Coulter). Libraries were sequenced single-end with 55 bp read length on an Illumina HiSeq 2500 platform in the DNA sequencing section (SQC) at the Okinawa Institute of Science and Technology Graduate University. Samples were de-multiplexed, filtered by quality, and trimmed to 55 bp using Trimmomatic [56].

Please cite this article in press as: Fischer et al., Socially Parasitic Ants Evolve a Mosaic of Host-Matching and Parasitic Morphological Traits, Current Biology (2020), https://doi.org/10.1016/j.cub.2020.06.078

QUANTIFICATION AND STATISTICAL ANALYSIS

de novo assembly of RAD loci

We used *ipyrad* v.0.7.13 [51] for *de novo* assembly of RAD loci. We used the default settings except for the following: max number of SNPs per locus set to 200; max number of indels per locus set to 200; restriction overhang explicitly set to null; min read length after adaptor trim set to 20. This process resulted in 447504 assembled loci.

Phylogenomic reconstruction

Using ipyrad's .loci output file as a starting point, we first trimmed down to the leading 25 bp for each locus, as mapping errors are concentrated toward the end of the locus. Of the 350 specimens included in the assembly, 63 were data deficient and were filtered out. RAD-sequencing tends to produce thousands to hundreds of thousands of loci, but with lots of missing data across specimens. In our tests, and in other studies examining phylogenomic reconstructions with similar data (e.g., see [69]), it is consistently clear that adding in more loci improves phylogenomic reconstruction even if they are only present in a few individuals, because any such loci present in at least four individuals can provide information about some internal nodes in the tree (even if not as much information as loci present across many individuals). This is especially true when missing data is hierarchically redundant and due to sequencing coverage rather than missing due to mutation-disruption (e.g., see [69]), as is the case in our dataset. Thus, we kept all loci that were present in at least four individuals (i.e., were potentially quartet informative) and used this alignment for the analysis (12,216,691 bp, mean bp per specimen 436,091, Std: 237,562, mean bp per species 935,083, std: 568,599, the mean per species is calculated as the consensus sequence of all specimens in a species).

Using this alignment, we inferred a Maximum Likelihood phylogeny as follows. We generated a starting tree set consisting of 20 parsimony and 20 random trees with RaxMLv8.2.4c [52] (options -y and -y -d respectively). We then ran ExaML v3.0.17 [53] with a PSR (GTRCAT) substitution model on the alignment and starting tree set and inferred an ML tree. For bootstrapping, we generated 100 bootstrapped alignments using the -f j option of RaxML and ran ExaML on each bootstrapped alignment to create a bootstrap tree set. We ran an a RaXML *a posteriori* bootstrap convergence assessment (-I autoMRE option) to determine if 100 replicates were sufficient, and found that they met the criterion. We also inferred an SVDquartets species tree implemented in tetrad v0.9.13, part of the ipyrad platform [69, 70]. Since tetrad does not accept multiple specimens per species, we used the specimen for each species with the most sequence data recovered. We ran tetrad on an alignment including 1137083 unlinked SNPs, derived from the same ipyrad run as the larger alignment. We inferred 420804 random quartets out of 4249575 possible quartets for the 102 taxa, and then conducted 100 non-parametric bootstrap replicates to assess support. The results from this analysis were congruent with the concatenated ML analysis, so we included the latter in the main text and the species tree in the dryad repository. Trees were visualized with iTOL [65] and FigTree [64].

We used BEAST v2.4.8 [54] to date the maximum likelihood topology and produce an ultrametric tree for comparative analysis. We first pruned the tree (in Figure 1) to one specimen per species (the specimen with the most data). For computational reasons, we did not use the full alignment but rather a subset of the loci by filtering out loci with high frequencies of missing data (e.g., keeping loci with greater than 20% or 30% specimen coverage in our alignment). We ran the analyses at different levels of missing data and found the resulting node ages were insensitive to this threshold, and thus used 20% (378,832 bp) threshold for the analysis we present. We first used partitionfinder (v2.1.1) [55] to select the nucleotide substitution model using on a smaller alignment (38 kbp) for computational reasons. The model scope included JC, K80, TRNEF, SYM, HKY, TRN, GTR, HKY+X, TRN+X, GTR+X, JC+G, K80+G, TRNEF+G, SYM+G, HKY+G, TRN+G, GTR+G, HKY+G+X, TRN+G+X, GTR+G+X; model_selection with AICc; search method greedy. This analysis selected a model of GTR+G+X which we used in the BEAST analysis. For calibration, we set the prior on the root node in our tree to be uniformly distributed within 7.4 – 15 MY, reflecting the range inferred by previous analyses (corresponding to the crown of the *Pheidole* old-world clade [17]). No relevant *Pheidole* fossils can date the different clades within our tree, which is why we used a secondary calibration from another study. Note, however, the absolute timescale of *Pheidole* evolution is an orthogonal issue to the main questions of this paper.

Linear measurements (2D morphology)

All linear measurements (in mm) were taken at 50x or 100x magnification, with Leica MZ12.5 and Leica M165C dissecting microscopes and an orthogonal crosshair micrometer, at an accuracy of about 0.01 mm to 0.005 mm. We took seven standard linear measurements (HW: head width; HL: head length; EL: eye length; MDL: mandible length; SL: scape length; WL: Weber's length = thorax length = proxy for body size; FL: hind femur length) (Figure S4A) from a total of 94 workers from 10 host-parasite species pairs (9 *P. lucida* group species and 9 host *Pheidole* species), as well as from 60 non-host Malagasy *Pheidole* species (222 specimens) for the permutation test (Figure 2D; Table S1). We also compared linear measurements of queens from 6 host-parasite species pairs (5 species each, and 8 and 21 specimens respectively) (Figure S3A).

X-ray micro-CT scanning and 3D geometric landmarks (3D morphology)

X-ray microtomography (micro-CT/μCT) 3D scans were created with a ZEISS Xradia 510 Versa, the ZEISS Scout and Scan Control System software, and processed with Amira (v6.5). One dry-mounted worker specimen per species was scanned to quantify variation in head and thorax shape across ten parasite-host pairs. In addition, we scanned eight non-host species randomly selected from the Malagasy *Pheidole* fauna for use in the permutation test (Figure 3D). Methods for micro-computed tomography scanning and 3D

surface reconstruction and processing follow lab protocols published in previous papers [71–73]. After creating hollow .ply surfaces in Meshlab (v2016.12) [57], we used *Checkpoint* (Stratovan, Davis, CA [58]) software to place a set of 13 landmarks and 4 sets of 5 sliding semi-landmarks on the head surface, and 29 landmarks on the thorax/mesosoma surface (Figure S4B). Landmarks and semi-landmark control points were designated based on criteria recommended in Zelditch et al. [74], evenly reflecting morphological shape while maintaining homology across *Pheidole* (and other Myrmicine genera). We aligned specimens using a generalized Procrustes analysis and extracted principal component (PC) axes describing shape variation in R using *geomorph* version 3.0.7 [61]. These PC axes were visualized in Figure 3 by warping a simplified and averaged *Pheidole* head and thorax to the extreme values of each axis, as in [75].

Comparative Analysis

We compared the effect of host morphology on the evolution of social parasite morphology through a series of phylogenetic generalized least-squares (PGLS) regressions. In each regression, we treated the host phenotype as the predictor variable and the parasite phenotype as the response variable. We log-transformed linear measurements and estimates of body size prior to comparison. For 3D shape characters, we used the principal component axes described above to compare characteristics of 3D shape in PGLS regressions.

We used the R package *geiger* to estimate an optimal lambda parameter [59, 76] and fit the PGLS model with the package *nlme* [60]. As one parasite species has been collected with multiple host species and another two parasites with the same host species on separate occasions, we repeated PGLS regressions for each of the four possible combinations of host phenotypes as predictor variables (Figures 2B and 3B). As an additional test, we also performed this analysis using a null model and non-parametric test by performing ordinary least-squares regressions between parasite and host phenotypes (OLS; not correcting for phylogeny), and compared the R^2 value of these regressions to those of 1000 simulated host-parasite pairs generated by shuffling non-host Madagascar *Pheidole* and parasites (Figures 2D and 3D). There were not enough pairs of queens to perform statistical analysis, so we simply checked visually if there was evidence of matching in a bivariate plot (there was not, see Figure S3).

One potential issue in comparing similarity in morphological shape between hosts and parasites is that it might be explained by allometric scaling of shape and size. To test for an effect of body size on body shape, we performed PGLS regressions between each trait and the centroid size of the thorax (a landmark-based estimate similar to Weber's Length), excluding the two parasite-host pairs where the parasites are not represented in our phylogeny. Of the eight PC axes analyzed for body shape, only PC1 ($R2 = 0.11$, $p < 0.05$) and PC2 ($R2 = 0.48$, $p < 0.001$) of thorax (mesosoma) shape showed significant allometric relationships (Figure 3C). To correct for the effect of body size on host-parasite similarity in shape and size, we repeated each of our PGLS regressions while including body size (thorax centroid) as a covariate (Figures 2C and 3C).

As an alternative method to differentiating between direct similarity in either 3D shape or individual measurements and indirect effects of shared body size allometries, we fit Structured Equation Models (SEMs) in the R package *lavaan* [62]. In each model, the regression of the parasite trait on the host trait was examined in the context of the body size relationship as a latent or indirect variable (Figure S2). Thus, this method assesses similarity in trait size or shape, while including correction for allometry in both the host and parasite, as well as the correlation in body size between the host and parasite. However, due to the relatively small sample size used in these models, their results should be interpreted with caution.

ADDITIONAL RESOURCES

We have not used any additional resources for this publication.

Current Biology, Volume *30*

Supplemental Information

Socially Parasitic Ants Evolve a Mosaic of Host-Matching and Parasitic Morphological Traits

Georg Fischer, Nicholas R. Friedman, Jen-Pan Huang, Nitish Narula, L. Lacey Knowles, Brian L. Fisher, Alexander S. Mikheyev, and Evan P. Economo

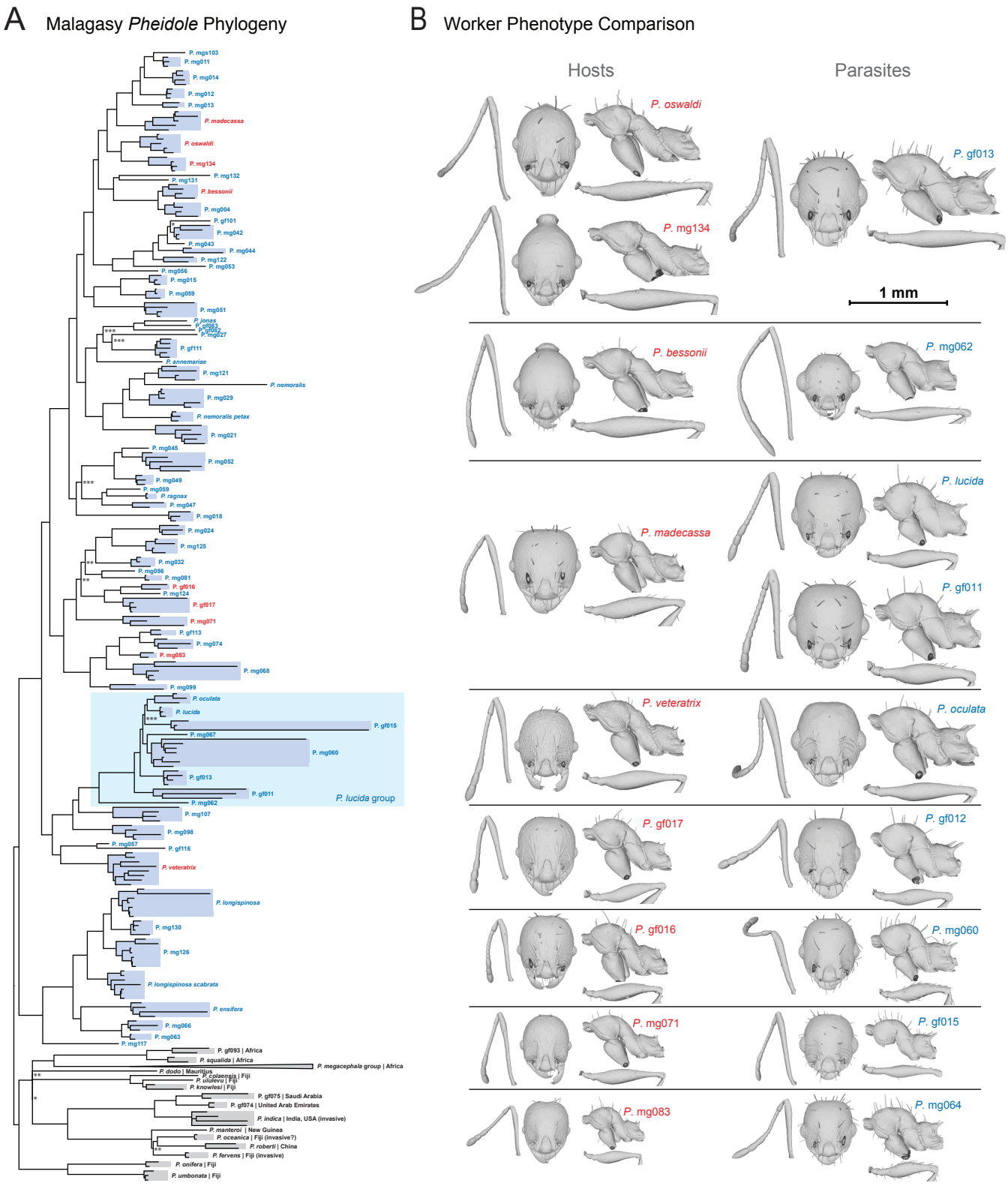

Figure S1. (A) Malgasy *Pheidole* phylogeny, including all sequenced specimens and outgroup. Related to Figure 1B. This tree was used as basis for the species tree (Figure 1). Taxa in blue and red represent endemic Malagasy species; the latter are host species, while the parasitic *P. lucida* group is highlighted in light blue. Outgroup taxa below are presented in black. Node support values are between 95 and 100 unless otherwise indicated [*<50, **50-80, ***80-95]. **(B) Phenotypic comparison of parasite-host pairs. Related to Figure 1C.** Parasitic (red) versus host species (blue), all depicted at the same scale (right antenna, head in full-face view, thorax in profile and left hind femur).

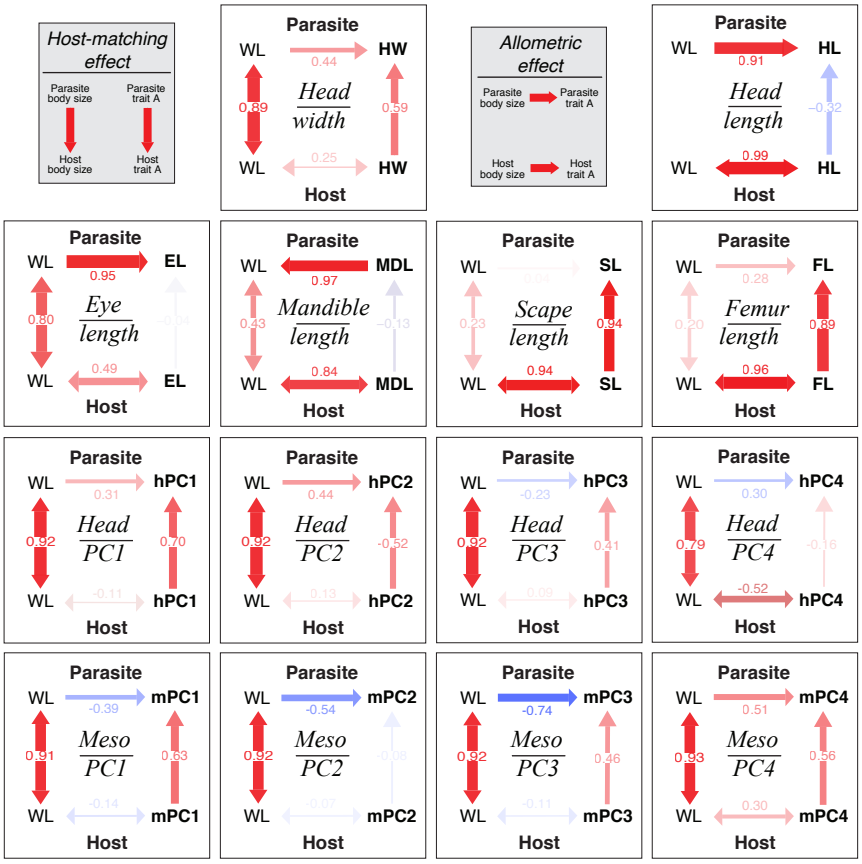

Figure S2. SEM path analyses results on possible allometry effects. Related to Figures 2 & 3. While body size (WL) is highly correlated between social parasite and host species, the linear measurements (HW, HL, EL, MDL, SL, FL) and head and thorax 3D-shape analyses (principal component axes: hPC = head, mPC = mesosoma) show a range of positive and negative interactions. The results indicate that the length of the antennae (SL), legs (FL) and (to a lesser degree) the width of the head (HW) evolve independently of pure size-allometry. 3D-shape analyses show a similar, albeit weaker, effect for some of the PC-axes (hPC1, mPC1, mPC4).

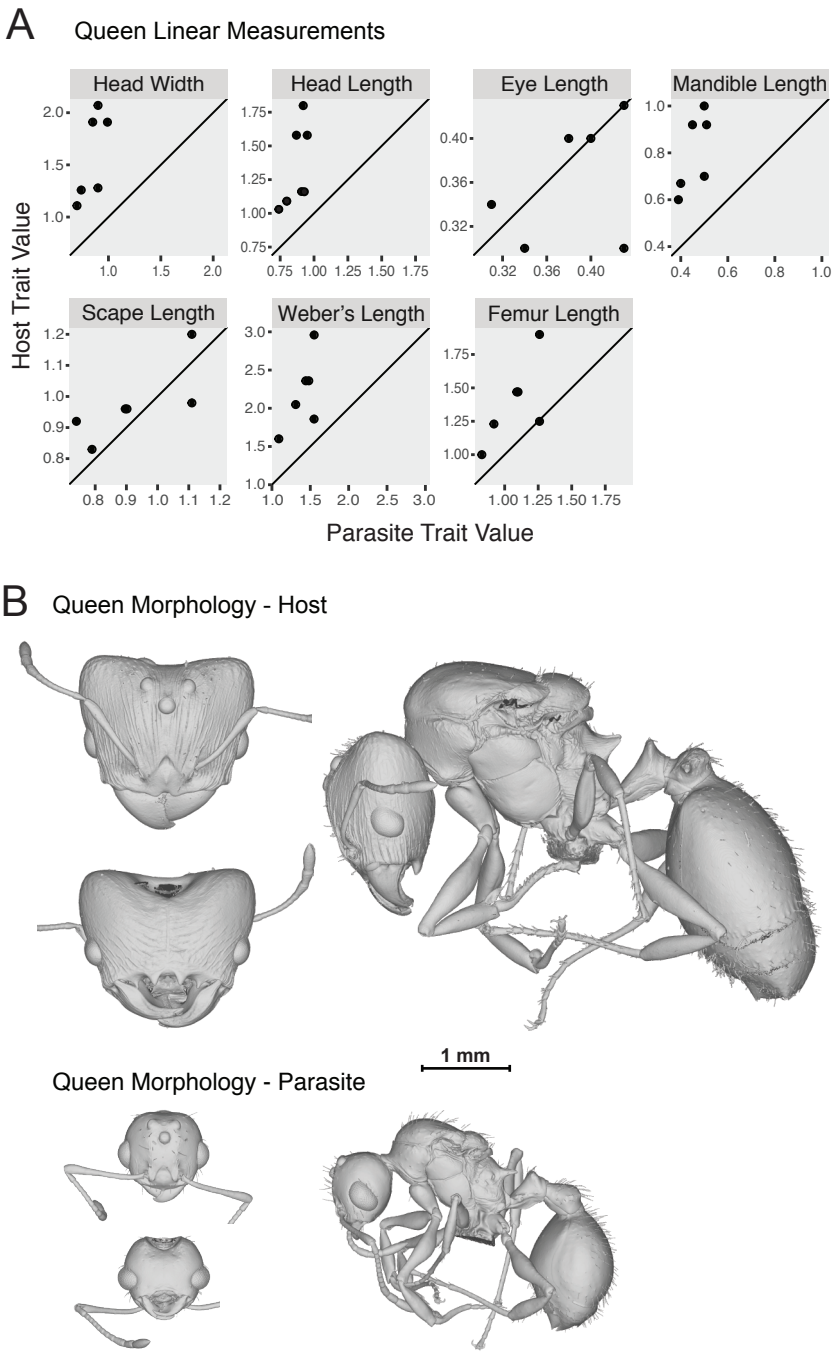

Figure S3. Queen morphology comparison. Related to Figure 2. (**A**) Weak correlation of individual linear measurements from queens of six species pairs, with host queens on the vertical and the parasite queens on the horizontal axis. Except for eye size, the host queens are significantly larger. (**B**) While the host (*P. madecassa*) shows a typical *Pheidole* queen morphology, the parasitic queen (*P*. gf011) shows a significant reduction in overall size and different body part proportions.

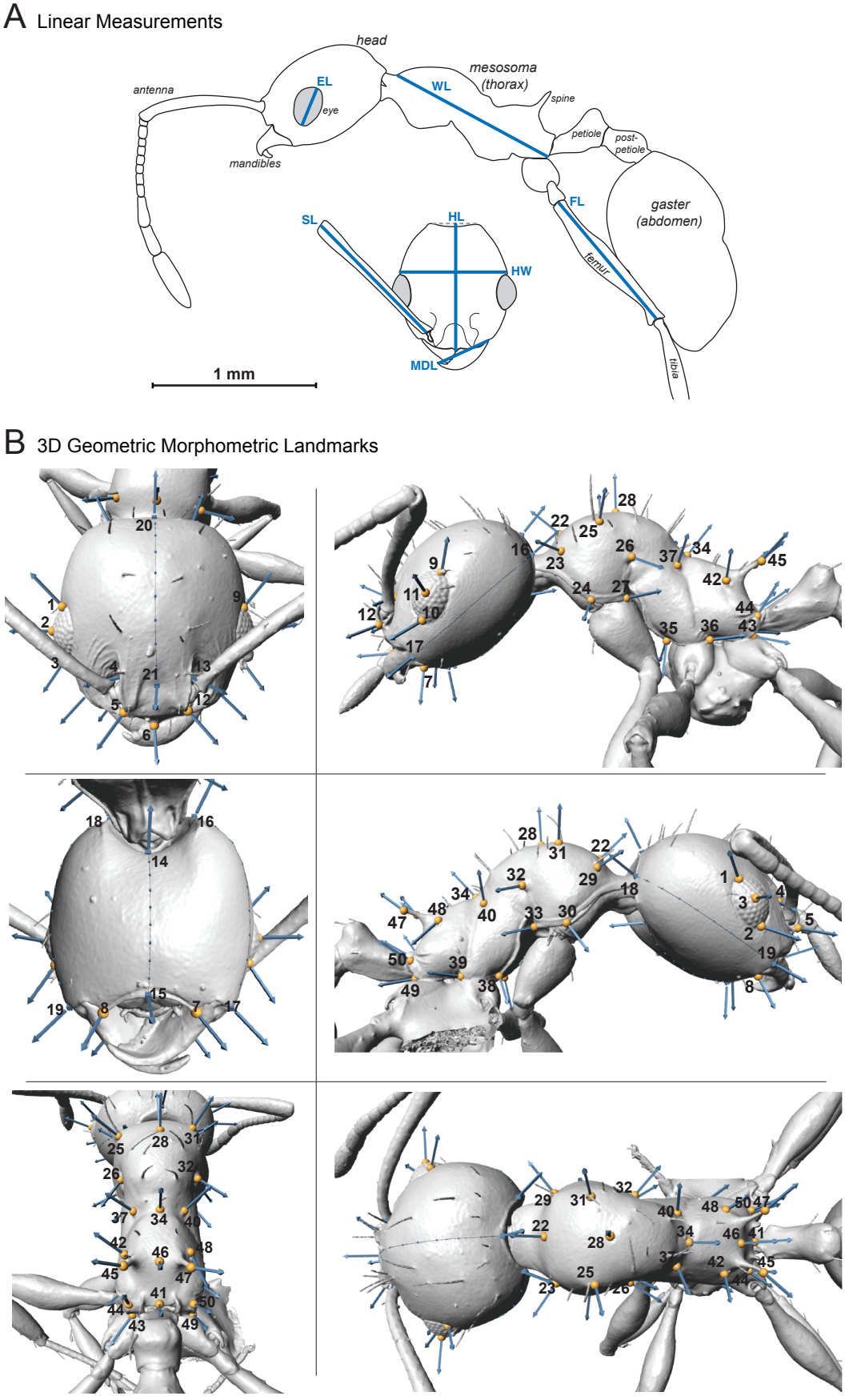

Figure S4. 2D measurements and 3D morphometry. Related to Figures 2 & 3. (**A**) Linear measurements: head and body of parasitic *Pheidole* gf011 worker in profile view, head in full-face view (HW: head width; HL: head length; EL: eye length; MDL: mandible length; SL: scape length; WL: Weber's length; FL: hind femur length). (**B**) 3D geometric morphometric landmarks placement on worker head and mesosoma (*P.* gf011).